

# UCLA

## UCLA Previously Published Works

### Title

Graphene growth with giant domains using chemical vapor deposition

### Permalink

<https://escholarship.org/uc/item/5sp3m7s3>

### Journal

CrystEngComm, 13(23)

### Authors

Yong, Virginia  
Hahn, H. Thomas

### Publication Date

2011-10-19

Peer reviewed

Cite this: *CrystEngComm*, 2011, **13**, 6933

www.rsc.org/crystengcomm

COMMUNICATION

## Graphene growth with giant domains using chemical vapor deposition

Virginia Yong\* and H. Thomas Hahn

Received 11th June 2011, Accepted 7th October 2011

DOI: 10.1039/c1ce05714f

**We report the first demonstration of the growth of giant graphene domains on platinum (Pt), which results in a uniform bilayer graphene film with domain sizes of millimetre scale. These giant graphene domains are attributed to the giant Pt grains attained in post-deposition annealed Pt thin films that exhibit a strong dependency on the Pt film thickness. Giant grains have been claimed to occur in other metallic materials under appropriate film thicknesses and processing conditions. Our findings demonstrate a route towards rational large-scale uniform graphene synthesis for applications in nanoelectronics and sensing.**

The experimental isolation of graphene in 2004<sup>1</sup> by micromechanical cleavage of highly oriented pyrolytic graphite (HOPG) has stimulated much experimental and theoretical research. Graphene is showing promise in a diverse range of applications, including sensors, transistors, spintronics, terahertz imaging, photovoltaics, membranes, batteries, capacitors, as well as composites and electrodes.<sup>2–7</sup> Conceptually introducing curvature and end-fusing into the flat sheets leads to one-dimensional (1D) carbon nanotubes (CNTs) or closed 0D fullerenes (such as C<sub>60</sub>) highlighting the distinct electronic and transport properties of this 2D structure,<sup>8–10</sup> as a consequence of the linear energy dispersion relation near the charge neutrality (Dirac) point in the electronic band structure. A half-integer quantum Hall effect was observed, due to the existence of both electron-like and hole-like Landau states at zero energy. Charge carriers in graphene behave as massless relativistic particles (Dirac fermions) and exhibit ballistic transport on the sub-micrometre scale at room temperature. An exceptionally high mobility (~25 000 to 200 000 cm<sup>2</sup>/Vs) of graphene has been experimentally<sup>8</sup> and theoretically<sup>9</sup> demonstrated, attributed to carrier confinement and coherence. In addition to its extraordinary electronic and transport properties, graphene exhibits a remarkable mechanical integrity and thermal stability. A measured Young's modulus of ~1 TPa, intrinsic strength of ~130 GPa, and thermal conductivity of ~5300 W/mK were recently reported.<sup>11,12</sup> Graphene films can be radically bent and stretched without affecting their optical and electronic properties, and it is the most flexible and stretchable transparent conducting material so far measured.<sup>13</sup> It is likely to play a major role in future nanodevices, quantum and flexible electronics.

Single-, bi- and few-layer (3 to <10) graphene can be distinguished as three different types of 2D crystals. Its electronic structure rapidly

evolves with the number of layers, approaching the 3D limit of graphite at 10 layers.<sup>14</sup> Single-layer graphene is a zero-gap semiconductor (or zero-overlap semimetal) with a linear Dirac-like spectrum around the Fermi energy. Bilayer graphene has a parabolic spectrum around the Fermi energy and shows a semimetallic behavior like graphite, with a band overlap of ~0.16 meV. Graphite is a semimetal with a band overlap of ~41 meV. Hence achieving homogeneous film thickness with large single-crystalline domains is particularly important. Whereas many papers have been written on single-layer graphene (perhaps because of its simplicity and the natural attraction of a one-atom-thick material), only a small fraction deals with multilayer (bi- and few-layer) graphene and the theoretical understanding and experimental exploration of multilayers is far behind the single layer. Nevertheless, multilayer graphene is equally interesting and unusual with a technological potential (both bilayer<sup>15</sup> and trilayer<sup>16</sup> exhibit a gate-tunable bandgap), perhaps larger than the single layer.<sup>17,18</sup> This is a fertile and opens field of research for the future.

In the last few years, a great deal of work has been dedicated to the development of chemical approaches to synthesize large-scale graphene, including 2D self-assembly of exfoliated graphene sheets<sup>19</sup> and reduced graphene oxides,<sup>20</sup> longitudinal unzipping of CNTs *via* solution-based oxidative process<sup>21</sup> and plasma etching,<sup>22</sup> and epitaxial growth and chemical vapor deposition (CVD) on silicon carbide (SiC),<sup>8,23</sup> ruthenium (Ru),<sup>24</sup> nickel (Ni)<sup>13,25</sup> and most recently on copper (Cu).<sup>26</sup> The electrical properties of graphene depend sensitively on the defect density of the graphene structures. The solution-processed graphene samples show relatively poor electrical properties owing to the structural defects formed during the vigorous exfoliation, oxidation or reduction processes. Epitaxial growth and CVD (on SiC, Ru, Ni, and Cu)<sup>8,13,23–26</sup> is an attractive alternative, which provides high-quality single-crystalline graphene sheets with very low defect density. The first epitaxial graphene layer interacts strongly with its substrate, whereas the second layer is almost completely detached and exhibits weak electronic coupling to its substrate hence retains the intrinsic electronic structure of graphene.<sup>24</sup> However, these epitaxial and transition-metal-catalyzed graphene growth (most often through thermal decomposition of hydrocarbons, and subsequent surface segregation of interstitial carbon atoms from the bulk metal owing to their temperature-dependent solubility) generally yield micrometre-sized graphene domains (~0.2–50 μm on SiC,<sup>8,23</sup> ~1–20 μm on Ni,<sup>13,25</sup> and ~100–200 μm on Ru.<sup>24</sup>) Achieving large graphene domains with uniform thickness remains the focus of current research efforts, primarily concentrating on the single-layer graphene growth.<sup>23–26</sup>

Department of Materials Science and Engineering, University of California, Los Angeles, CA, 90095, USA. E-mail: hyong@ucla.edu

Observations of the structural coherence of graphene across steps (it has been shown that graphene can bridge across gaps, thus forming a continuous film) suggest that the sizes of graphene domains will not be limited by the substrate step spacing.<sup>24,25</sup> Nonetheless, the morphology of graphene domains with constant thickness resembles the morphology (shape and size of the grains) of the substrates used for graphene growth.<sup>23,25</sup> Therefore, achieving homogeneous film thickness with large graphene domains requires control of the grain size and texture of the substrates that develop during deposition and post-deposition annealing processes. Grain growth in thin films may appear as normal or abnormal grain growth.<sup>27</sup> Normal grain growth often develops a log-normal grain size distribution and is frequently obstructed by grain boundary grooving, leading to stagnation at a final grain size of two to three times the film thickness.<sup>28</sup> Abnormal grain growth results in a bimodal grain size distribution in the course of the growth process. Grain growth in this case usually stops when the abnormally growing grains coalesce. The final average grain diameter may then be many times the film thickness.<sup>29</sup> An abnormal giant grain growth in the millimetre range was reported in silver (Ag)<sup>30</sup> and platinum (Pt)<sup>31</sup> thin films. Depending on film thickness, normal grain growth (thickness below 0.6  $\mu\text{m}$ ), abnormal grain growth (thickness between 1.0 and 1.5  $\mu\text{m}$ ) and the growth of giant grains (thickness above 2.0  $\mu\text{m}$ ) were observed in post-deposition annealed Ag thin films.<sup>30</sup> The final grain size reached millimetres,<sup>30,31</sup> which corresponds to more than 1000 times the film thickness or 10 000 times the initial grain size.

In this communication, we report the first demonstration of the growth of giant graphene domains on Pt, which results in homogeneous bilayer graphene with large single-crystalline domain sizes in the range of millimetre scale. The observed giant graphene domains are attributed to the giant grains attained in post-deposition annealed Pt thin films. 2.3  $\mu\text{m}$  thick Pt films were deposited on (100) silicon wafers with a 100 nm thermal SiO<sub>2</sub> layer using direct current (DC) magnetron sputtering (Plasma Sciences CrC-150 sputtering system, FTM-2000 rate/thickness monitor, Torr International, Inc.) at a deposition rate of 3.1  $\text{\AA s}^{-1}$  under high vacuum conditions (base pressure:  $\sim 10^{-5}$  Torr, partial argon pressure during deposition:  $5 \times 10^{-3}$  Torr). Post-sputtered thermal annealing was performed in a tube furnace (Lindberg 55035 tube furnace, Eurotherm 847 temperature controller, Thermo Electron Corporation; base pressure:  $\sim 1$  Torr) with a mixed gas flow of hydrogen (H<sub>2</sub>) and argon (Ar), H<sub>2</sub> : Ar = 160 : 160 standard cubic centimetres per minute (sccm), at 900 °C for 1 h. Graphene was grown by CVD of methane (CH<sub>4</sub>), CH<sub>4</sub> : H<sub>2</sub> : Ar = 15 : 500 : 600 sccm, under a constant pressure of 915 Torr at 1000 °C for 7 min. The graphene growth occurred due to the surface segregation of interstitial carbon atoms from the bulk Pt film as observed for other transition metals, such as Ni and Cu. During the exposure of the Pt surface to a CH<sub>4</sub> and H<sub>2</sub> gas mixture, the Pt and carbon atoms (from thermal decomposition of hydrocarbons) form a solid solution. Since the solubility of carbon in Pt is temperature-dependent, carbon atoms precipitate as a graphene layer on the Pt surface upon cooling of the sample. Unlike Ni and Cu, which are easily oxidized into nickel and copper oxide, Pt is not oxidized due to its inertness, which might reduce irregularity of the surface. In addition, graphene on Pt stands out as the system with the weakest graphene-metal interaction among a broader group of 3d, 4d, and 5d transition metals.<sup>32</sup> The weak substrate coupling of graphene on Pt might lead to distinct electronic properties from other transition metal supported graphene systems. Single-layer graphene growth on

Pt has been demonstrated recently.<sup>33,34</sup> Here, we report bi-layer graphene growth on Pt, which is equally interesting and unusual with a technological potential (both bilayer<sup>15</sup> and trilayer<sup>16</sup> exhibit a gate-tunable bandgap) perhaps larger than the single layer.<sup>17,18</sup>

The morphology (size and shape), domain sizes, surface coverage, uniformity, number of layers, and defect density of as-deposited graphene on the annealed 2.3  $\mu\text{m}$  thick Pt films were characterized on an optical microscope (Zeiss polarizing optical microscope, Axioplan 2 imaging), a scanning electron microscope (JEOL 6500F field emission SEM), a high resolution transmission electron microscope (JEOL 2100F field emission HRTEM operated at 200 kV accelerating voltage), an atomic force microscope (Veeco Multimode DI AFM with Nanoscope V controller), and by Raman spectroscopy (Renishaw inVia Raman microscope).

Optical photograph at 100X revealed giant graphene domains in millimetre sizes, Fig. 1(a). A close-up view of the graphene film at 250X under SEM shows a homogenous and defect-free graphene film, Fig. 1(b). No grain boundaries or line defects were observed at this scale of magnification. Further examinations on the graphene surface at a higher magnification of 500X revealed the presence of pinholes or voids with sizes of  $\sim 1 \mu\text{m}$  at some locations, inset of Fig. 1(b). The observed pinholes or voids in the microstructure were likely associated with the defects on the Pt films formed during the sputtering or post-sputtered annealing processes. Fig. 1(c) and (d) show typical TEM and AFM images of the bilayer graphene film with thickness of  $\sim 1 \text{ nm}$ .

Fig. 2(a) shows the Raman spectrum of as-deposited graphene film on Pt taken at room temperature at an excitation wavelength of 514.5 nm with a 50X objective. The two most intense features are a G band at  $\sim 1584 \text{ cm}^{-1}$  due to the doubly degenerate E<sub>2g</sub> mode at the

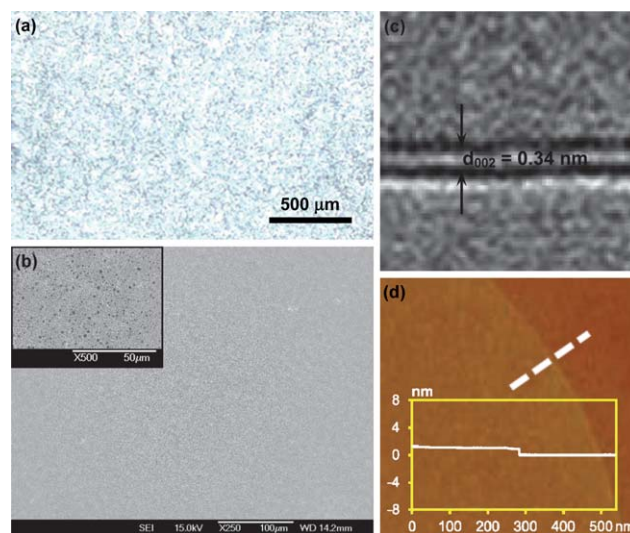


**Fig. 1** (a) Optical photograph at 100X showing a typical giant domain size in millimetre scale. (b) SEM micrograph at 250X did not reveal any grain boundaries or line defects, consistent with the observed millimetre-sized domains shown in (a). Inset: A close-up view of the graphene surface at 500X showing the presence of pinholes or voids, which is likely associated with the defects on Pt film formed during the sputtering or post-sputtered annealing processes. (c) TEM showing a typical micrograph of the bilayer graphene film. (d) AFM image of bilayer graphene transferred onto SiO<sub>2</sub>/Si substrate. Inset: Cross section height profile measured along the dashed line revealing a layer thickness of  $\sim 1 \text{ nm}$ .

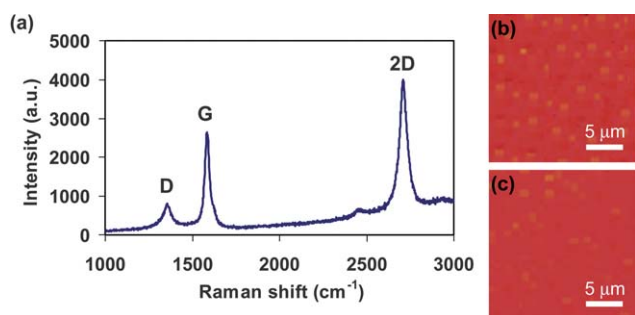


**Fig. 2** (a) Raman spectrum of as-deposited graphene film on Pt showing the D band at  $\sim 1355\text{ cm}^{-1}$ , the G band at  $\sim 1584\text{ cm}^{-1}$ , and the 2D band at  $\sim 2710\text{ cm}^{-1}$ . The spectrum is recorded at an excitation wavelength of  $514.5\text{ nm}$  and normalized to the peak intensity of the 2D line ( $\sim 2710\text{ cm}^{-1}$ ). (b) and (c) Raman maps of the FWHM's of 2D band and  $I_{2D}/I_G$  ratios, respectively.

zone center, and a second-order D\* (2D) band at  $\sim 2710\text{ cm}^{-1}$  due to two phonons with opposite momentum in the highest optical branch near the K point. A D band, identified with disorder-induced first-order scattering, was observed at  $\sim 1355\text{ cm}^{-1}$ . The observed pinholes/voids (defects induced by the underlying Pt substrate) on the graphene surface at 500X, the inset of Fig. 1(b), are presumed to be responsible for the presence of the D band. The 2D band results from a double resonance process that links the phonon wave vectors to the electronic band structure, and its line shape can serve as a fingerprint of the electronic structure of single-, bi-, or few-layer graphene. The 2D band exhibits a broadened peak with full width at half maximum (FWHM) of  $50\text{ cm}^{-1}$  and blue-shifted of  $20\text{ cm}^{-1}$  with respect to that of single-layer graphene (FWHM of  $\sim 25\text{ cm}^{-1}$  at  $\sim 2690\text{ cm}^{-1}$ ), a clear signature for bilayer graphene.<sup>35,36</sup> The center position, width, and intensity ratios of the 2D and G bands ( $I_{2D}/I_G$ ) remain constant over the entire giant graphene domains several square millimetres in size, Fig. 2(b) and (c), which indicates that a uniform bilayer graphene film was formed on the entire giant Pt grains.

In summary, we report the first demonstration of giant-domains graphene growth on platinum. The observed giant graphene domains are resulted from the giant Pt grains. Giant grains have been claimed to occur in other metallic materials under appropriate film thicknesses and processing conditions.<sup>27,31</sup> Our findings demonstrate a route towards rational large-scale uniform graphene synthesis for applications in nanoelectronics and sensing.

The authors would like to thank the National Science Foundation and Department of Energy for financial support.

## References

- 1 K. S. Novoselov, A. K. Geim, S. V. Morozov, D. Jiang, Y. Zhang, S. V. Dubonos, I. V. Grigorieva and A. A. Firsov, Electric field effect in atomically thin carbon films, *Science*, 2004, **306**(5296), 666–669.
- 2 R. Van Noorden, The graphene challenge, *Chem. World*, 2008, **5**(4), 56–59.
- 3 V. Yung and J. M. Tour, Theoretical efficiency of nanostructured graphene-based photovoltaics, *Small*, 2010, **6**(2), 313–318.
- 4 H. J. Jiang, Chemical preparation of graphene-based nanomaterials and their applications in chemical and biological sensors, *Small*, 2011, **7**(17), 2413–2427.
- 5 X. Huang, X. Y. Qi, F. Boey and H. Zhang, Graphene-based composites, *Chem. Soc. Rev.*, 2012, DOI: 10.1039/C1CS15078B.

- 6 H. Bai, C. Li and G. Q. Shi, Functional Composite Materials Based on Chemically Converted Graphene, *Adv. Mater.*, 2011, **23**(9), 1089–1115.
- 7 X. Huang, Z. Y. Yin, S. X. Wu, X. Y. Qi, Q. Y. He, Q. C. Zhang, Q. Y. Yan, F. Boey and H. Zhang, Graphene-Based Materials: Synthesis, Characterization, Properties, and Applications, *Small*, 2011, **7**(14), 1876–1902.
- 8 C. Berger, Z. M. Song, X. B. Li, X. S. Wu, N. Brown, C. Naud, D. Mayou, T. B. Li, J. Hass, A. N. Marchenkov, E. H. Conrad, P. N. First and W. A. de Heer, Electronic confinement and coherence in patterned epitaxial graphene, *Science*, 2006, **312**(5777), 1191–1196.
- 9 S. V. Morozov, K. S. Novoselov, M. I. Katsnelson, F. Schedin, D. C. Elias, J. A. Jaszczak and A. K. Geim, Giant intrinsic carrier mobilities in graphene and its bilayer, *Phys. Rev. Lett.*, 2008, **100**(1), 016602.
- 10 Y. B. Zhang, Y. W. Tan, H. L. Stormer and P. Kim, Experimental observation of the quantum Hall effect and Berry's phase in graphene, *Nature*, 2005, **438**(7065), 201–204.
- 11 C. Lee, X. D. Wei, J. W. Kysar and J. Hone, Measurement of the elastic properties and intrinsic strength of monolayer graphene, *Science*, 2008, **321**(5887), 385–388.
- 12 A. A. Balandin, S. Ghosh, W. Z. Bao, I. Calizo, D. Teweldebrhan, F. Miao and C. N. Lau, Superior thermal conductivity of single-layer graphene, *Nano Lett.*, 2008, **8**(3), 902–907.
- 13 K. S. Kim, Y. Zhao, H. Jang, S. Y. Lee, J. M. Kim, K. S. Kim, J. H. Ahn, P. Kim, J. Y. Choi and B. H. Hong, Large-scale pattern growth of graphene films for stretchable transparent electrodes, *Nature*, 2009, **457**(7230), 706–710.
- 14 B. Partoens and F. M. Peeters, From graphene to graphite: Electronic structure around the K point, *Phys. Rev. B: Condens. Matter Mater. Phys.*, 2006, **74**(7), 075404.
- 15 Y. B. Zhang, T. T. Tang, C. Girit, Z. Hao, M. C. Martin, A. Zettl, M. F. Crommie, Y. R. Shen and F. Wang, Direct observation of a widely tunable bandgap in bilayer graphene, *Nature*, 2009, **459**(7248), 820–823.
- 16 M. F. Craciun, S. Russo, M. Yamamoto, J. B. Oostinga, A. F. Morpurgo and S. Thruha, Trilayer graphene is a semimetal with a gate-tunable band overlap, *Nat. Nanotechnol.*, 2009, **4**(6), 383–388.
- 17 A. K. Geim, Graphene: Status and Prospects, *Science*, 2009, **324**(5934), 1530–1534.
- 18 A. H. C. Neto, F. Guinea, N. M. R. Peres, K. S. Novoselov and A. K. Geim, The electronic properties of graphene, *Rev. Mod. Phys.*, 2009, **81**(1), 109–162.
- 19 X. L. Li, G. Y. Zhang, X. D. Bai, X. M. Sun, X. R. Wang, E. Wang and H. J. Dai, Highly conducting graphene sheets and Langmuir–Blodgett films, *Nat. Nanotechnol.*, 2008, **3**(9), 538–542.
- 20 G. Eda, G. Fanchini and M. Chhowalla, Large-area ultrathin films of reduced graphene oxide as a transparent and flexible electronic material, *Nat. Nanotechnol.*, 2008, **3**(5), 270–274.
- 21 D. V. Kosynkin, A. L. Higginbotham, A. Sinititskii, J. R. Lomeda, A. Dimiev, B. K. Price and J. M. Tour, Longitudinal unzipping of carbon nanotubes to form graphene nanoribbons, *Nature*, 2009, **458**(7240), 872–876.
- 22 L. Y. Jiao, L. Zhang, X. R. Wang, G. Diankov and H. J. Dai, Narrow graphene nanoribbons from carbon nanotubes, *Nature*, 2009, **458**(7240), 877–880.
- 23 K. V. Emtsev, A. Bostwick, K. Horn, J. Jobst, G. L. Kellogg, L. Ley, J. L. McChesney, T. Ohta, S. A. Reshanov, J. Rohrl, E. Rotenberg, A. K. Schmid, D. Waldmann, H. B. Weber and T. Seyller, Towards wafer-size graphene layers by atmospheric pressure graphitization of silicon carbide, *Nat. Mater.*, 2009, **8**(3), 203–207.
- 24 P. W. Sutter, J. I. Flege and E. A. Sutter, Epitaxial graphene on ruthenium, *Nat. Mater.*, 2008, **7**(5), 406–411.
- 25 A. Reina, X. T. Jia, J. Ho, D. Nezich, H. B. Son, V. Bulovic, M. S. Dresselhaus and J. Kong, Large area, few-layer graphene films on arbitrary substrates by chemical vapor deposition, *Nano Lett.*, 2009, **9**(1), 30–35.
- 26 X. S. Li, W. W. Cai, J. H. An, S. Kim, J. Nah, D. X. Yang, R. Piner, A. Velamakanni, I. Jung, E. Tutuc, S. K. Banerjee, L. Colombo and R. S. Ruoff, Large-area synthesis of high-quality and uniform graphene films on copper foils, *Science*, 2009, **324**(5932), 1312–1314.
- 27 C. V. Thompson and R. Carel, Stress and grain growth in thin films, *J. Mech. Phys. Solids*, 1996, **44**(5), 657–673.

- 28 H. J. Frost, C. V. Thompson and D. T. Walton, Simulation of thin film grain structures—I. Grain growth stagnation, *Acta Metall. Mater.*, 1990, **38**(8), 1455–1462.
- 29 H. J. Frost, C. V. Thompson and D. T. Walton, Simulation of thin film grain structures—II. Abnormal grain growth, *Acta Metall. Mater.*, 1992, **40**(4), 779–793.
- 30 J. Greiser, P. Mullner and E. Arzt, Abnormal growth of “giant” grains in silver thin films, *Acta Mater.*, 2001, **49**(6), 1041–1050.
- 31 D. S. Lee, D. Y. Park, H. J. Woo, S. H. Kim, J. Ha and E. Yoon, Preferred orientation controlled giant grain growth of platinum thin films on SiO<sub>2</sub>/Si substrates, *Jpn. J. Appl. Phys.*, 2001, **40**(1AB), L1–L3.
- 32 A. B. Preobrajenski, M. L. Ng, A. S. Vinogradov and N. Martensson, Controlling graphene corrugation on lattice-mismatched substrates, *Phys. Rev. B: Condens. Matter Mater. Phys.*, 2008, **78**(7), 073401.
- 33 B. J. Kang, J. H. Mun, C. Y. Hwang and B. J. Cho, Monolayer graphene growth on sputtered thin film platinum, *J. Appl. Phys.*, 2009, **106**(10), 104309.
- 34 P. Sutter, J. T. Sadowski and E. Sutter, Graphene on Pt(111): Growth and substrate interaction, *Phys. Rev. B: Condens. Matter Mater. Phys.*, 2009, **80**(24), 245411.
- 35 A. C. Ferrari, J. C. Meyer, V. Scardaci, C. Casiraghi, M. Lazzeri, F. Mauri, S. Piscanec, D. Jiang, K. S. Novoselov, S. Roth and A. K. Geim, Raman spectrum of graphene and graphene layers, *Phys. Rev. Lett.*, 2006, **97**(18), 187401.
- 36 L. M. Malard, M. A. Pimenta, G. Dresselhaus and M. S. Dresselhaus, Raman spectroscopy in graphene, *Phys. Rep.-Rev. Sect. Phys. Lett.*, 2009, **473**(5–6), 51–87.